JOM 23115

Synthesis, structure and hydrogenation of η^3-benzyl diphosphine complexes of rhodium and iridium

Michael D. Fryzuk, David H. McConville and Steven J. Rettig

Department of Chemistry, University of British Columbia, 2036 Main Mall, Vancouver, B.C. V6T 1Z1 (Canada)

(Received May 30, 1991; in revised form July 23, 1992)

Abstract

The preparation of (COD)Rh(η^3-CH_2Ph) is described starting from $[(COD)Rh]_2(\mu\text{-}Cl)_2$ by the addition of either $Zn(CH_2Ph)_2$ or $Mg(CH_2Ph)_2(THF)_2$. The addition of the bulky chelating diphosphines $^tBu_2P(CH_2)_3P^tBu_2$, $^iPr_2P(CH_2)_3P^iPr_2$, $^iPr_2P(CH_2)_2P^iPr_2$, $^iPr_2PCH_2P^iPr_2$ and $Cy_2PCH_2PCy_2$ to (COD)Rh(η^3-CH_2Ph) yields the coordinatively unsaturated, four-coordinate rhodium complexes of the form $P_2Rh(\eta^3\text{-}CH_2Ph)$. Iridium complexes of the form $P_2Ir(\eta^3\text{-}CH_2Ph)$ (where $P_2 = {}^tBu_2P(CH_2)_3P^tBu_2$ and $^iPr_2P(CH_2)_3P^iPr_2$) can be prepared from $[P_2Ir]_2(\mu\text{-}Cl)_2$ and $Zn(CH_2Ph)_2$ or $Mg(CH_2Ph)_2(THF)_2$. Reaction of the benzyl complexes with H_2 (1 atm) yields binuclear hydride derivatives of varying composition depending on the chelate ring size of the coordinated diphosphine. For the diphosphines with only a single methylene in the backbone, binuclear hexahydride complexes are formed in which the diphosphine is binucleating. The X-ray structure of $\{^iPr_2P(CH_2)_3P^iPr_2\}Rh(\eta^3\text{-}CH_2Ph)$ shows a square planar geometry about rhodium with alternating single and double bonds in the η^3-coordinated benzyl fragment. Crystals of {1,3-bis(diisopropylphosphino)propane}rhodium(η^3-benzyl) are monoclinic, $a = 10.540(3)$, $b = 15.030(9)$, $c = 14.858(5)$ Å, $\beta = 92.91(3)°$, $Z = 4$, $D_c = 1.329$ g cm^{-3}, space group $P2_1/n$. The structure was solved by the Patterson method and was refined by full-matrix least-squares procedures to $R = 0.036$ and $R_w = 0.043$ for 4152 reflections with $I \geq 3\sigma(I)$.

1. Introduction

While benzyl complexes of rhodium are suggested to be key intermediates in the decarbonylation of certain acid chlorides [1], few such complexes have actually been isolated [2–5]. In general, the synthesis of η^3-benzyl complexes can be achieved in several ways, for example, insertion of styrene into a metal hydride bond [3], deprotonation of coordinated hexamethylbenzene [2], protonation of coordinated styrene [6], metathesis [7], halide abstraction from a benzyl metal halide complex [8], and oxidative addition of benzylhalide to a metal [9]. The weak bonding interaction of the phenyl portion of the η^3-benzyl fragment leads to a rapid exchange process (suprafacial *vs.* antarafacial) which can be observed on the NMR time scale by variable temperature ^1H NMR spectroscopy [10].

In this paper, we report the high yield preparation of the simple rhodium η^3-benzyl complex, (COD)Rh(η^3-CH_2Ph) (**1**), by the reaction of $Zn(CH_2Ph)_2$ or $Mg(CH_2Ph)_2(THF)_2$ with $[(COD)Rh]_2(\mu\text{-}Cl)_2$. This complex is a useful precursor to diphosphine rhodium η^3-benzyl derivatives by simple displacement of the COD ligand. The resultant diphosphine complexes react rapidly with H_2 to give polyhydrides of various composition depending on the diphosphine used.

Previously, we have described the synthesis [11,12] of the coordinatively unsaturated dimers of the general form, $[P_2Rh]_2(\mu\text{-}H)_2$ (**I**), incorporating bulky chelating diphosphines. The coordinatively unsaturated nature of these dimers has led to a diverse and rich chemistry [13–16].

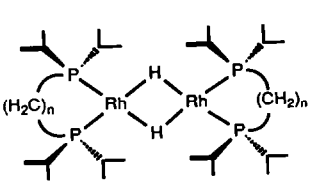

I

n = 2, 3, 4

We have now extended this work to the bulky, one-carbon backbone diphosphines $^iPr_2PCH_2P^iPr_2$ and $Cy_2PCH_2PCy_2$; what emerges from this investigation is the facile formation of a binuclear hexahydride com-

Correspondence to: Dr. M.D. Fryzuk.

0022-328X/93/$6.00

plex, $[P_2RhH_3]_2$, where $P_2 = {}^iPr_2PCH_2P{}^iPr_2$ or $Cy_2PCH_2PCy_2$. Apparently the small chelate ring size of these coordinated diphosphine ligands precludes formation of the dihydride bridged complexes found for those diphosphines that generate larger chelate rings.

2. Experimental section

2.1. General information

All manipulations were performed under prepurified nitrogen in a Vacuum Atmospheres HE-553-2 glovebox equipped with a MO-40-2H purifier or in standard Schlenk-type glassware on a vacuum line. $RhCl_3 \cdot xH_2O$ and $IrCl_3 \cdot xH_2O$ were obtained from Johnson–Matthey and used as received to prepare $[(COD)Rh]_2(\mu\text{-}Cl)_2$ (COD = 1,5-cyclooctadiene) [17] and $[(COE)_2Ir]_2(\mu\text{-}Cl)_2$ (COE = cyclooctene) [18], respectively. The description "reactor bomb" refers to a cylindrical, thick-walled Pyrex vessel equipped with a 9 mm Teflon needle valve and a ground glass joint for attachment to a vacuum line.

Toluene, hexanes, pentane and tetrahydrofuran (THF) were dried by refluxing over sodium-benzophenone ketyl followed by distillation under argon. Deuterated benzene (C_6D_6) and toluene (C_7D_8) were purchased from Aldrich, dried over activated 4 Å molecular sieves, vacuum transferred and freeze–pump–thawed three times prior to use.

Microanalyses of these air- and moisture-sensitive compounds were expertly performed by Mr. Peter Borda of this department. ^1H NMR spectra were recorded on either a Varian XL-300 (299.94 MHz) or a Bruker WH-400 (400.00 MHz) spectrometer and referenced to C_6D_5H or $C_6D_5CD_2H$ set at 7.15 ppm and 2.09 ppm, respectively. $^{13}C\{^1H\}$ and $^{31}P\{^1H\}$ NMR spectra were recorded on a Varian XL-300 spectrometer (75.43 MHz and 121.42 MHz, respectively). The $^{31}P\{^1H\}$ NMR spectra were referenced to external $P(OMe)_3$ set at 141.0 ppm and $^{13}C\{^1H\}$ to C_6D_6 set at 128.0 ppm. $^1H\{^{31}P\}$ NMR were recorded on a Bruker AMX-500 (500 MHz) spectrometer.

Dibenzylzinc $Zn(CH_2Ph)_2$ and bis(tetrahydrofuran)dibenzylmagnesium $Mg(CH_2Ph)_2(THF)_2$ [19], 1,3-bis(di-tert-butylphosphino)propane (dtbpp) and 1,3-bis(diisopropylphosphino)propane (dippp) [20], 1,2-bis(diisopropylphosphino)ethane (dippe) [12], bis(diisopropylphosphino)methane (dippm) [21] were prepared according to the literature. Bis(dicyclohexylphosphino) methane (dcypm) was prepared from $Cl_2PCH_2PCl_2$ [21] and cyclohexyl Grignard ($C_6H_{11}MgCl$) in Et_2O as described below. The hydride dimers $[(dippp)Rh]_2(\mu\text{-}H)_2$ [11] and $[(dippe)Rh]_2(\mu\text{-}H)_2$ [12] were identified spectroscopically by comparison with authentic samples prepared by published routes. Hydrogen gas used in hydrogenation reactions was purified by passing through a glass tower packed with MnO on vermiculite and 4 Å molecular sieves separated by a plug of glass wool.

2.2. $Cy_2PCH_2PCy_2$

To a mechanically stirred solution of $C_6H_{11}MgCl$ (429 ml, 1 M) in Et_2O (500 ml) at 0°C in a 1 l, 3-necked flask was added dropwise an ether (100 ml) solution of $Cl_2PCH_2PCl_2$ (15.00 g, 53.6 mmol) over 2 h. The mixture was stirred for an additional 2 h. The excess Grignard was destroyed by adding 500 ml of degassed H_2O (saturated with NH_4Cl) dropwise at 0°C. The ethereal layer was separated from the aqueous layer and dried with sodium sulfate (10 g of Na_2SO_4). The ether was removed under vacuum to yield 13.2 g of crude $Cy_2PCH_2PCy_2$ (61%). The product can be recrystallized from ether at −40°C. $^{31}P\{^1H\}$ NMR (C_6D_6): δ −11.1 (s) ppm.

2.3. $(COD)Rh(\eta^3\text{-}CH_2Ph)$ (1)

2.3.1. Using $Zn(CH_2Ph)_2$

To a suspension containing $[(COD)Rh]_2(\mu\text{-}Cl)_2$ (250 mg, 0.507 mmol) in toluene (50 ml) was added dropwise a solution of $Zn(CH_2Ph)_2$ (126 mg, 0.509 mmol) in toluene (10 ml) over 1 min. The initially yellow solution turned dark orange as $ZnCl_2$ precipitated. The mixture was stirred for 4 h followed by removal of the toluene under vacuum and taking up of the solid in pentane (50 ml). The mixture was stirred for 20 min and then filtered through a medium porosity frit. Concentration of the solution *in vacuo* to 10 ml followed by cooling to −40°C yielded 245 mg (80%) of orange crystalline **1**. Larger scale reactions gave lower yields using $Zn(CH_2Ph)_2$. The complex can be stored for several months at −40°C. Anal. Found: C, 59.46; H, 6.36. $C_{15}H_{19}Rh$ calc.: C, 59.61; H, 6.34%. ^1H NMR (C_6D_6): δ 7.08 (t, *meta*, 2H); 6.72 (t, *para*, 1H); 5.71 (d, *ortho*, 2H); 4.68 (s, =C*H*, 2H); 3.77 (s, =C*H*, 2H); 2.12 (s, CH_2Ph, 2H); 2.0–1.7 (m, CH_2 of COD, 8H) ppm. $^{13}C\{^1H\}$ NMR (C_6D_6): δ 132.4 (C_m of Ph); 123.1 (C_{ipso} of Ph); 121.8 (C_p of Ph); 109.7 (C_o of Ph); 87.3 (d, =*C*H, ^1J(C,Rh) = 9.6 Hz); 73.0 (d, =*C*H, ^1J(C,Rh) = 15.2 Hz); 38.4 (d, *C*H_2Ph, ^1J(C,Rh) = 10.9 Hz); 32.2 (*C*H_2 of COD); 30.6 (*C*H_2 of COD) ppm.

2.3.2. Using $Mg(CH_2Ph)_2(THF)_2$

To a solution containing $[(COD)Rh]_2(\mu\text{-}Cl)_2$ (1.103 g, 2.23 mmol) in THF (100 ml) was added dropwise a solution of $Mg(CH_2Ph)_2(THF)_2$ (0.785 g, 2.24 mmol) in THF (10 ml). The initially yellow solution turned dark orange. After 4 h the THF was removed under vacuum and the solid was taken up in pentane (75 ml). The

mixture was stirred for 20 min and then filtered through a medium porosity frit. Removal of the solvent yielded 1.240 g (92%) of **1**.

2.4. *(dtbpp)Rh(η^3-CH_2Ph) (2)*

To a solution containing **1** (142 mg, 0.469 mmol) in hexanes (10 ml) was added dropwise a solution of dtbpp (156 mg, 0.469 mmol) in hexanes (5 ml). The solution turned deep red from the initial orange colour. The solution was stirred for 1 h followed by filtration. The volume was reduced *in vacuo* to 10 ml and cooled to −40°C to yield 175 mg (71%) of red crystalline **2**. Anal. Found: C, 59.58; H, 9.49. $C_{26}H_{49}P_2Rh$ calc.: C, 59.31; H, 9.38%. ^{1}H NMR (C_6D_6): δ 7.21 (t, *meta*, 2H); 6.84 (t, *para*, 1H); 6.04 (d, *ortho*, 2H); 2.31 (d, CH_2Ph, 2H, ^3J(H,P) = 6.2 Hz); 1.68 (m, CH_2 ligand, 2H); 1.36 (m, CH_2 ligand, 4H); 1.26 (d, CH_3 of ligand, 18H); 1.03 (d, CH_3 of ligand, 18H) ppm. ^{31}P{^{1}H} NMR (C_6D_6); 61.5 (dd, P_A, ^1J(P,Rh) = 266 Hz; ^2J(P,P′) = 29 Hz); 51.4 (dd, P_B, ^1J(P,Rh) = 173 Hz; ^2J(P′,P) = 29 Hz). ^{13}C{^{1}H} NMR (C_6D_6): δ 132.3 (C_m of Ph); 121.4 (C_{ipso} of Ph); 120.9 (C_p of Ph); 109.2 (d, C_o of Ph, ^2J(C,P) = 7.2 Hz); 38.4 (*C*(CH$_3$)$_3$); 38.6 (*C*(CH$_3$)$_3$); 37.0 (d, *C*H$_2$Ph, ^1J(C,Rh) = 9.5 Hz); 31.1 (d, *C*H$_3$ of ligand); 30.6 (d, *C*H$_3$ of ligand); 24.1 (ligand); 23.4 (ligand); 22.8 (ligand) ppm.

2.5. *(dippp)Rh(η^3-CH_2Ph) (3)*

The preparation of **3** is analogous to that of **2**. Compound **3** was obtained as red crystals in 85% yield. Anal. Found: C, 56.08; H, 8.77. $C_{22}H_{41}P_2Rh$ calc.: C, 56.17; H, 8.78%. ^{1}H NMR (C_6D_6): δ 7.24 (t, *meta*, 2H); 6.63 (t, *para*, 1H); 5.87 (d, *ortho*, 2H); 2.25 (d, CH_2Ph, 2H, ^3J(H,P) = 7.1 Hz); 1.92 (d of sept, C*H*(CH$_3$)$_2$, 2H); 1.68 (m, PCH_2, 2H); 1.64 (d of sept, C*H*(CH$_3$)$_2$, 2H); 1.26 (m, PCH_2, 2H); 1.23 (m, PCH$_2$CH_2, 2H); 1.12 (dd, CH(CH_3)$_2$, 6H); 1.04 (dd, CH(CH_3)$_2$, 6H); 0.96 (dd, CH(CH_3)$_2$, 6H); 0.85 (dd, CH(CH_3)$_2$, 6H) ppm. ^{31}P{^{1}H} NMR (C_6D_6): δ 48.3 (dd, P_A, ^1J(P,Rh) = 242 Hz; ^2J(P,P′) = 40.8 Hz); 33.9 (dd, P_B, ^1J(P,Rh) = 172 Hz; ^2J(P′,P) = 40.8 Hz) ppm. ^{13}C{^{1}H} (C_6D_6): δ 132.2 (C_m of Ph); 119.1 (C_{ipso} of Ph); 117.8 (C_p of Ph); 105.1 (d, C_o of Ph, ^2J(C,P) = 7.7 Hz); 34.8 (ddd, *C*H$_2$Ph, ^1J(C,Rh) = 9.1 Hz; ^2J(C,P) = 32.1 Hz; ^2J(C,P′) = 2.5 Hz); 29.8 (d, CH(*C*H$_3$)); 25.6 (d, CH(*C*H$_3$)); 23.9 (d, ligand backbone); 21.1 (d, *C*H(CH$_3$)); 20.9 (d, *C*H(CH$_3$)); 20.5 (d, ligand backbone); 20.2 (d, ligand backbone); 20.0 (dd, CH(*C*H$_3$)); 19.3 (d, CH(*C*H$_3$)) ppm.

2.6. *(dippe)Rh(η^3-CH_2Ph) (4)*

See preparation of **2** for experimental details. Compound **4** was obtained in 80% yield as deep orange crystals. Anal. Found: C, 55.35; H, 8.76. $C_{21}H_{39}P_2Rh$ calc.: C, 55.27; H, 8.61%. ^{1}H NMR (C_6D_6): δ 7.29 (t, *meta*, 2H); 6.57 (t, *para*, 1H); 5.91 (d, *ortho*, 2H); 2.47 (d, CH_2Ph, 2H, ^3J(H,P) = 7.5 Hz); 1.88 (d of sept, C*H*(CH$_3$)$_2$, 2H); 1.69 (d of sept, C*H*(CH$_3$)$_2$, 2H); 1.19 (m, PCH_2, 4H); 1.07 (dd, CH(CH_3)$_2$, 6H); 0.92–0.77 (m, CH(CH_3)$_2$, 18H) ppm. ^{31}P{^{1}H} NMR (C_6D_6): δ 97.9 (dd, P_A, ^1J(P,Rh) = 245 Hz; ^2J(P,P′) = 20.5 Hz); 91.0 (dd, P_B, ^1J(P,Rh) = 177 Hz; ^2J(P′,P) = 20.5 Hz) ppm. ^{13}C{^{1}H} NMR (C_6D_6): δ 132.5 (C_m of Ph); 119.1 (C_{ipso} of Ph); 118.1 (C_p of Ph); 105.6 (d, C_o of Ph, ^2J(C,P) = 8.7 Hz); 32.5 (dd, *C*H$_2$Ph; ^1J(C,Rh) = 8.7 Hz; ^2J(C,P) = 33.9 Hz); 28.0 (dd, *C*H(CH$_3$)$_2$); 25.7 (d, *C*H(CH$_3$)$_2$); 23.7 (ddd, P*C*H$_2$); 21.7 (ddd, P*C*H$_2$); 20.1 (d, CH(*C*H$_3$)$_2$); 19.8 (d, CH(*C*H$_3$)$_2$); 19.1 (d, CH(*C*H$_3$)$_2$); 18.9 (d, CH(*C*H$_3$)$_2$) ppm.

2.7. *(dcypm)Rh(η^3-CH_2Ph) (5)*

The preparation of **5** is analogous to that of **2**. Compound **5** was isolated as orange plates in 92% yield. Anal. Found: C, 64.03; H, 9.08. $C_{32}H_{53}P_2Rh$ calc.: C, 63.78; H, 8.86%. ^{1}H NMR (C_6D_6): δ 7.41 (t, *meta*, 2H); 6.54 (t, *para*, 1H); 5.96 (d, *ortho*, 2H); 2.61 (t, PCH_2P, 2H); 2.41 (d, CH_2Ph, 2H, ^3J(H,P) = 6.6 Hz); 2.1–1.1 (br m, ligand resonances, 44H) ppm. ^{31}P{^{1}H} NMR (C_6D_6): δ 13.7 (dd, P_A, ^1J(P,Rh) = 221 Hz; ^2J(P,P′) = 77 Hz); 1.0 (dd, P_B, ^1J(P,Rh) = 148 Hz; ^2J(P′,P) = 77 Hz) ppm. ^{13}C{^{1}H} NMR (C_6D_6): δ 132.8 (C_m of Ph); 120.1 (C_{ipso} of Ph); 118.0 (C_p of Ph); 106.3 (d, C_o of Ph, ^2J(C,P) = 9.5 Hz); 37.5 (dd, P*C*H$_2$P); 36.7 (dd, *C*H$_2$Ph, ^1J(C,Rh) = 4.1 Hz; ^2J(C,P) = 13.2 Hz); 30.3; 30.2; 29.9; 29.8; 27.7; 27.6; 27.5; 27.4; 26.7 (overlapping cyclohexyl carbons).

2.8. *(dippm)Rh(η^3-CH_2Ph) (6)*

See preparation of **2** for experimental details. Compound **6** was obtained in 77% yield as deep red–orange crystals. Anal. Found: C, 54.46; H, 8.41. $C_{20}H_{37}P_2Rh$ calc.: C, 54.30; 8.43%. ^{1}H NMR (C_6D_6): δ 7.35 (t, *meta*, 2H); 6.55 (t, *para*, 1H); 5.90 (d, *ortho*, 2H); 2.38 (d t, PCH_2P, 2H); 2.36 (d, CH_2Ph, 2H, ^3J(H,P) = 6.9 Hz); 1.77 (d of sept, C*H*(CH$_3$)$_2$, 2H); 1.64 (d of sept, C*H*(CH$_3$)$_2$, 2H); 1.11 (dd, CH(CH_3)$_2$, 6H); 1.08 (dd, CH(CH_3)$_2$, 6H); 0.95 (dd, CH(CH_3)$_2$, 6H); 0.91 (dd, CH(CH_3)$_2$, 6H) ppm. ^{31}P{^{1}H} NMR (C_6D_6): δ 23.4 (dd, P_A, ^1J(P,Rh) = 222 Hz; ^2J(P,P′) = 77 Hz); 10.8 (dd, P_B, ^1J(P,Rh) = 149 Hz; ^2J(P′,P) = 77 Hz) ppm. ^{13}C{^{1}H} NMR (C_6D_6): δ 132.8 (C_m of Ph); 120.2 (C_{ipso} of Ph); 117.9 (C_p of Ph); 106.5 (d, C_o of Ph, ^2J(C,P) = 9.6 Hz); 35.1 (dd, P*C*H$_2$P); 29.1 (dd, *C*H$_2$Ph, ^1J(C,Rh) = 9.2 Hz; ^2J(C,P) = 36.9 Hz); 26.8 (ddd, *C*H(CH$_3$)$_2$); 26.4 (dd, *C*H(CH$_3$)); 19.9 (d, CH(*C*H$_3$)$_2$); 19.8 (d, CH(*C*H$_3$)$_2$); 19.5 (d, CH(*C*H$_3$)$_2$); 19.3 (d, CH(*C*H$_3$)$_2$)

ppm. Mol. wt. (cryoscopic in benzene): found 450, calc.: 442.

2.9. [(dtbpp)Rh]$_2$(μ-H)$_2$ (7)

In a 350 ml reactor bomb equipped with a stir bar was added **2** (176 mg, 0.334 mmol) in toluene (50 ml). The solution was degassed three times and the vessel cooled to −196°C. Hydrogen was then added to 1 atm and the inlet valve closed. The solution was warmed to room temperature and stirred for 24 h. The toluene was removed under vacuum and the product extracted with 30 ml of THF. The deep green solution was filtered, concentrated to 15 ml and cooled to −40°C to yield 78 mg (54%) of green crystalline **7**. Anal. Found: C, 61.21; H, 11.69. $C_{38}H_{86}P_4Rh_2$ calc.: C, 60.94; H, 11.57%. ^{1}H NMR (C_6D_6): δ 1.81 (m, PCH_2, 8H); 1.48 (m, PCH$_2$CH_2, 4H); 1.39 (d, PC(CH_3)$_3$, 72H); −8.79 (quin of t, RhHRh, 2H, ^1J(H,Rh) = 9.6 Hz; ^2J(H,P) = 22.2 Hz) ppm. ^{31}P{^{1}H} (C_6D_6): δ 69.8 (br d, ^1J(P,Rh) = 145 Hz) ppm.

2.10. [(dippp)Rh]$_2$(μ-H)$_2$ (8)

The preparation of **8** is analogous to **7** with the exception that the product was isolated from toluene/hexanes. Compound **8** was isolated in 84% yield as green crystals. ^{1}H NMR (C_6D_6): δ 1.82 (d of sept, CH(CH$_3$)$_2$, 8H); 1.60 (dd, CH(CH_3)$_2$, 24H); 1.21 (dd, CH(CH_3)$_2$, 24H); 0.95 (m, ligand backbone, 12H); −6.61 (quin of t, RhHRh, 2H) ppm. ^{31}P{^{1}H} NMR (C_6D_6): δ 50.2 (d of m, ^1J(P,Rh) = 160 Hz).

2.11. [(dippe)Rh]$_2$(μ-H)$_2$ (9)

The preparation of **9** is analogous to **7** with the exception that the product was isolated from toluene/hexanes. Compound **9** was isolated as green crystals in 66% yield. ^{1}H NMR (C_6D_6): δ 1.83 (d of sept, CH(CH$_3$)$_2$), 8H); 1.40 (dd, CH(CH_3)$_2$, 24H); 1.11 (dd, CH(CH_3)$_2$, 24H); 1.04 (br d, ligand backbone, 8H); −4.81 (quin of t, RhHRh, 2H) ppm. ^{31}P{^{1}H} NMR (C_6D_6): δ 104.7 (d of m, ^1J(P,Rh) = 160 Hz).

2.12. [RhH$_2$]$_2$(μ-H)$_2$(μ-dcypm)$_2$ (10)

In a sealable NMR tube was dissolved **5** (30 mg, 0.049 mmol) in C_7D_8 (0.4 ml). The tube was cooled to −196°C and hydrogen introduced to 1 atm. The tube was sealed and the solution warmed to room temperature as the deep red–black hydride formed. Only one compound is formed as shown by ^{31}P NMR spectroscopy. ^{1}H NMR (C_6D_6): δ 2.21 (br m, PCH_2, 4H); 1.80, 1.62, 1.41 (m, ligand resonances, 88H); −10.90 (m, RhHRh, 2H); −14.73 (m, RhH, 4H) ppm. ^{31}P{^{1}H} NMR (C_6D_6): δ 65.8 (d of m, ^1J(P,Rh) = 107 Hz).

2.13. [RhH$_2$]$_2$(μ-H)$_2$(μ-dippm)$_2$ (11)

In a 350 ml reactor bomb equipped with a stir bar was added **6** (75 mg, 0.169 mmol) in 25 ml pentane. The solution was degassed three times and the vessel cooled to −196°C. Hydrogen was then added to 1 atm and the inlet valve closed. The solution was warmed to room temperature and stirred for 4 h. The color of the solution turned deep red–black instantly. The reaction is quantitative by ^{31}P NMR spectroscopy. Compound **11** can be recrystallized from pentane at −40°C and is stable in the solid state. Anal. Found: C, 44.41; H, 9.51. $C_{38}H_{86}P_4Rh_2$ calc.: C, 44.08; H, 9.39%. ^{1}H NMR (C_6D_6): δ 1.91 (br m, PCH_2, 4H); 1.88 (d of sept, CH(CH$_3$)$_2$, 8H); 1.25 (dd, CH(CH_3)$_2$, 24H); 1.20 (dd, CH(CH_3)$_2$, 24H); −10.92 (m, RhHRh, 2H); −14.88 (m, RhH, 4H) ppm. ^{31}P{^{1}H} NMR (C_6D_6): δ 74.3 (d of m, ^1J(P,Rh) = 107 Hz) ppm. ^{1}H{^{31}P} NMR (C_6D_6): δ 1.91 (s, PCH_2, 4H); 1.88 (sept, CH(CH$_3$)$_2$, 8H); 1.25 (d, CH(CH_3)$_2$, 24H); 1.20 (d, CH(CH_3)$_2$, 24H); −10.92 (quin of t, RhHRh, 2H, ^2J(H,H′) = 4.5 Hz; ^1J(H,Rh) = 24.5 Hz); −14.88 (m, RhH, 4H) ppm. Mol. wt. (cryoscopic in benzene): found 722; calc.: 708.

2.14. [(dtbpp)Ir]$_2$(μ-Cl)$_2$ (12)

To a stirred suspension of [(COE)$_2$Ir]$_2$(μ-Cl)$_2$ (389 mg, 0.434 mmol) in hexanes (25 ml) was added slowly a solution of dtbpp (289 mg, 0.869 mmol) in 10 ml of hexanes. The color of the solution changed instantly from orange to deep red as the solution became homogeneous. After a few seconds the solution began to precipitate a red powder. The volume was reduced to 10 ml of hexanes and the mixture cooled to −40°C for 24 h. The red powder was collected on a fine porosity frit and washed with 5 ml of cold hexanes to yield 447 mg (92%) of **12**. The product was dried under vacuum for 6 h on a vacuum line to remove residual COE. The product is extremely oxygen-sensitive and should be stored under nitrogen at −40°C. This sensitivity thwarted all attempts to obtain accurate microanalysis of this product. The powder was sufficiently pure for metathetical reactions. ^{1}H NMR (C_6D_6): δ 1.51 (d, PC(CH_3)$_3$); 1.35 (m, PCH_2); 1.21 (m, PCH$_2$CH_2) ppm. ^{31}P{^{1}H} NMR (C_6D_6): δ 14.69 (s) ppm.

2.15. [(dippp)Ir]$_2$(μ-Cl)$_2$ (13)

See preparation of **12** for experimental details. Compound **13** was obtained in 90% yield as an orange powder. Again **13** is extremely oxygen-sensitive and should be stored under nitrogen at −40°C. ^{1}H NMR (C_6D_6): δ 2.13 (d of sept, PCH(CH$_3$)$_2$); 1.54 (dd, PCH(CH_3)$_2$; 1.18 (dd, PCH(CH_3)$_2$); 0.96 (m, PCH_2 and PCH$_2$CH_2) ppm. ^{31}P{^{1}H} NMR (C_6D_6): δ 11.37 (s) ppm.

2.16. (dtbpp)Ir(η^3-CH_2Ph) (14)

To a stirred suspension of **12** (184 mg, 0.164 mmol) in toluene (25 ml) was added dropwise a solution of $Zn(CH_2Ph)_2$ (41 mg, 0.166 mmol) in hexanes (10 ml). The colour of the solution changed from red to orange as $ZnCl_2$ precipitated. The stirring was continued for 24 h after which time the mixture was filtered through a medium porosity frit. Concentration of the solution to 10 ml and cooling to −40°C overnight yielded 145 mg of orange crystalline **14** (72%). Anal. Found: C, 50.31; H, 7.59. $C_{26}H_{49}P_2Ir$ calc.: C, 50.71; H, 8.02%. ^1H NMR (C_6D_6): δ 7.15 (t, *meta*, 2H); 6.68 (t, *para*, 1H); 6.03 (d, *ortho*, 2H); 2.49 (t, CH_2Ph, 2H, $^3J(H,P)$ = 2.3 Hz); 1.70 (m, CH_2 ligand, 2H); 1.48 (m, CH_2 ligand, 4H); 1.25 (br s, CH_3 of ligand, 18H); 1.15 (br s, CH_3 of ligand, 18H) ppm. $^{31}P\{^1H\}$ NMR (C_6D_6): δ 39.8 (br s, P_A); 36.4 (br s, P_B) ppm. $^{13}C\{^1H\}$ NMR (C_6D_6): δ 132.4 (C_m of Ph); 120.9 (C_{ipso} of Ph); 120.7 (C_p of Ph); 109.2 (d, C_o of Ph, $^2J(C,P)$ = 7.2 Hz); 38.6 ($C(CH_3)_3$); 38.4 ($C(CH_3)_3$); 37.1 (d, CH_2Ph, $^1J(C,Rh)$ = 9.2 Hz); 31.1 (d, CH_3 of ligand); 30.6 (d, CH_3 of ligand); 24.2 (ligand); 23.4 (ligand); 22.9 (ligand).

2.17. (dippp)Ir(η^3-CH_2Ph) (15)

The preparation of **15** is analogous to that of **14**. Compound **15** was obtained as red crystals in 70% yield. ^1H NMR (C_6D_6): δ 7.18 (t, *meta*, 2H); 6.54 (t, *para*, 1H); 5.84 (d, *ortho*, 2H); 2.38 (d, CH_2Ph, 2H, $^3J(H,P)$ = 7.0 Hz); 2.04 (d of sept, $CH(CH_3)_2$, 2H); 1.82 (d of sept, $CH(CH_3)_2$, 2H); 1.69 (m, PCH_2, 2H); 1.51 (m, PCH_2, 2H); 1.21 (m, PCH_2CH_2, 2H); 1.11 (dd, $CH(CH_3)_2$, 6H); 1.05 (dd, $CH(CH_3)_2$, 6H); 0.98 (dd, $CH(CH_3)_2$, 6H); 0.87 (dd, $CH(CH_3)_2$, 6H) ppm. $^{31}P\{^1H\}$ NMR (C_6D_6): δ 27.0 (d, P_A, $^2J(P,P')$ = 11.2 Hz); 21.4 (d, P_B, $^2J(P',P)$ = 11.2 Hz) ppm. $^{13}C\{^1H\}$ (C_6D_6): δ 132.2 (C_m of Ph); 119.1 (C_{ipso} of Ph); 117.8 (C_p of Ph); 105.1 (d, C_o of Ph, $^2J(C,P)$ = 7.7 Hz); 34.8 (ddd, CH_2Ph, $^1J(C,Rh)$ = 9.1 Hz; $^2J(C,P)$ = 32.1 Hz; $^2J(C,P')$ = 2.5 Hz); 29.8 (d, $CH(CH_3)$); 25.6 (d, $CH(CH_3)$); 23.9 (d, ligand backbone); 21.2 (d, $CH(CH_3)$); 20.9 (d, $CH(CH_3)$); 20.5 (d, ligand backbone); 20.2 (d, ligand backbone); 20.0 (dd, $CH(CH_3)$); 19.3 (d, $CH(CH_3)$) ppm.

2.18. X-Ray crystallographic analysis of (dippp)Rh(η^3-CH_2Ph)

Crystallographic data appear in Table 1. The bond distances and bond angles are listed in Tables 2 and 3, respectively. The final unit-cell parameters were obtained by least-squares on the setting angles for 25 reflections with $2\theta = 29.3$–$37.0°$. The intensities of three standard reflections, measured every 200 reflections throughout the data collection, showed a linear decay of 6.8%. The data were processed [22] and corrected for Lorentz and polarization effects, decay, and absorption (empirical, based on azimuthal scans for three reflections). A total of 7325 reflections with $2\theta \leq 60°$ was collected on a Rigaku AFC6S diffractometer, 7084 were unique (R_{int} = 0.028) and those 4152 with $I \geq 3\sigma(I)$ were employed in the solution and refinement of the structure.

The structure was solved by conventional heavy atom methods, the coordinates of the Rh and P atoms being determined from the Patterson function and those of the remaining non-hydrogen atoms from a subsequent

TABLE 1. Crystallographic data [a]

Compound	(dippp)Rh(η^3-benzyl)
Formula	$C_{22}H_{41}P_2Rh$
FW	470.42
Colour, habit	Orange prism
Crystal size (mm)	0.25×0.40×0.45
Crystal system	Monoclinic
Space group	$P2_1/n$
a (Å)	10.540(3)
b (Å)	15.030(9)
c (Å)	14.858(5)
β (°)	92.91(3)
V (Å^3)	2351(2)
Z	4
D_c (g/cm^3)	1.329
$F(000)$	992
Radiation	Mo
Wavelength (Å)	0.71069
μ (cm^{-1})	8.52
Transmission factors	0.73–1.00
Scan type	ω–2θ
Scan range (deg in ω)	1.35 + 0.35 tan θ
Scan speed (deg/min)	32
Data collected	$\pm h, +k, +l$
$2\theta_{max}$ (°)	60
Crystal decay (%)	6.8
Total no. of reflections	7325
No. of unique reflections	7084
R_{int}	0.028
No. of reflections with $I \geq 3\sigma(I)$	4152
No. of variables	238
R	0.036
R_w	0.043
GOF	1.33
Max Δ/σ (final cycle)	0.06
Residual density (e/Å^3)	−0.74 + 1.20 (both near Rh)

[a] Temperature 294 K, Rigaku AFC6S diffractometer, graphite monochromator, takeoff angle 6.0°, aperture 6.0×6.0 mm^2 at a distance of 285 mm from the crystal, stationary background counts at each end of the scan (scan/background time ratio 2:1), $\sigma^2(F^2) = [S^2(C+4B)+(0.04F^2)^2]/Lp^2$ (S = scan speed, C = scan count, B = normalized background count), function minimized $\Sigma w(|F_o| - |F_c|)^2$ where $w = 4F_o^2/\sigma^2(F_o^2)$, $R = \Sigma ||F_o| - |F_c|| / \Sigma |F_o|$, $R_w = (\Sigma w(|F_o| - |F_c|)^2/\Sigma w|F_o|^2)^{1/2}$, and GOF = $[\Sigma(|F_o| - |F_c|)^2/(m-n)]^{1/2}$. Values given for R, R_w, and GOF are based on those reflections with $I \geq 3\sigma(I)$.

TABLE 2. Final atomic coordinates and equivalent isotropic thermal parameters

Atom	x	y	z	B_{eq}
Rh(1)	0.42648(2)	0.23824(2)	0.16881(2)	2.95(1)
P(1)	0.61338(8)	0.29422(6)	0.21265(6)	3.66(4)
P(2)	0.3887(1)	0.16739(6)	0.29851(6)	3.79(4)
C(1)	0.6854(4)	0.2621(3)	0.3233(3)	5.0(2)
C(2)	0.6501(4)	0.1706(3)	0.3571(3)	5.4(2)
C(3)	0.5158(4)	0.1647(3)	0.3892(3)	5.3(2)
C(4)	0.7396(4)	0.2639(3)	0.1350(3)	4.7(2)
C(5)	0.6275(4)	0.4171(3)	0.2212(3)	5.0(2)
C(6)	0.3494(4)	0.0480(3)	0.2819(3)	5.1(2)
C(7)	0.2552(4)	0.2095(3)	0.3629(3)	5.2(2)
C(8)	0.7562(5)	0.1631(3)	0.1334(3)	6.5(3)
C(9)	0.8682(4)	0.3106(4)	0.1517(4)	7.6(3)
C(10)	0.6129(5)	0.4629(3)	0.1300(4)	6.7(3)
C(11)	0.5320(5)	0.4538(3)	0.2846(3)	6.3(2)
C(12)	0.4523(5)	0.0018(3)	0.2319(3)	6.5(2)
C(13)	0.3155(6)	−0.0054(4)	0.3649(4)	8.1(3)
C(14)	0.1271(5)	0.1948(4)	0.3134(3)	7.0(3)
C(15)	0.2743(5)	0.3089(4)	0.3815(4)	7.1(3)
C(16)	0.4289(4)	0.2919(3)	0.0354(3)	4.2(2)
C(17)	0.3533(3)	0.2132(2)	0.0300(2)	3.5(1)
C(18)	0.2407(3)	0.2083(2)	0.0783(2)	3.7(1)
C(19)	0.1682(4)	0.1304(3)	0.0773(3)	4.7(2)
C(20)	0.2081(5)	0.0564(3)	0.0342(3)	5.4(2)
C(21)	0.3231(5)	0.0575(3)	−0.0074(3)	5.5(2)
C(22)	0.3937(4)	0.1324(3)	−0.0093(2)	4.5(2)

TABLE 3. Bond lengths (Å) with estimated standard deviations in parentheses

Atom	Atom	Distance	Atom	Atom	Distance
Rh(1)	P(1)	2.210(1)	C(4)	C(9)	1.535(6)
Rh(1)	P(2)	2.255(1)	C(5)	C(10)	1.520(6)
Rh(1)	C(16)	2.141(4)	C(5)	C(11)	1.516(6)
Rh(1)	C(17)	2.197(3)	C(6)	C(12)	1.514(7)
Rh(1)	C(18)	2.362(3)	C(6)	C(13)	1.529(6)
P(1)	C(1)	1.840(4)	C(7)	C(14)	1.521(7)
P(1)	C(4)	1.862(4)	C(7)	C(15)	1.531(7)
P(1)	C(5)	1.857(4)	C(16)	C(17)	1.426(5)
P(2)	C(3)	1.852(4)	C(17)	C(18)	1.419(5)
P(2)	C(6)	1.856(4)	C(17)	C(22)	1.422(5)
P(2)	C(7)	1.853(4)	C(18)	C(19)	1.398(5)
C(1)	C(2)	1.516(6)	C(19)	C(20)	1.360(6)
C(2)	C(3)	1.518(6)	C(20)	C(21)	1.389(6)
C(4)	C(8)	1.525(6)	C(21)	C(22)	1.351(6)

difference Fourier synthesis. The non-hydrogen atoms were refined with anisotropic thermal parameters and the hydrogen atoms were fixed in idealized positions (C–H = 0.98 Å, $B_H = 1.2B_{\text{bonded atom}}$). Neutral atom scattering factors and anomalous dispersion corrections for all atoms were taken from the *International Tables for X-Ray Crystallography* [23]. Final atomic coordinates and equivalent isotropic thermal parame-

TABLE 4. Bond angles (°) with estimated standard deviations in parentheses

Atom	Atom	Atom	Angle	Atom	Atom	Atom	Angle
P(1)	Rh(1)	P(2)	96.99(4)	P(1)	C(4)	C(9)	116.1(3)
P(1)	Rh(1)	C(16)	94.4(1)	C(8)	C(4)	C(9)	110.8(4)
P(1)	Rh(1)	C(17)	127.4(1)	P(1)	C(5)	C(10)	112.7(3)
P(1)	Rh(1)	C(18)	160.27(9)	P(1)	C(5)	C(11)	110.5(3)
P(2)	Rh(1)	C(16)	168.5(1)	C(10)	C(5)	C(11)	110.4(4)
P(2)	Rh(1)	C(17)	130.71(9)	P(2)	C(6)	C(12)	110.4(3)
P(2)	Rh(1)	C(18)	102.7(1)	P(2)	C(6)	C(13)	117.3(3)
C(16)	Rh(1)	C(17)	38.4(1)	C(12)	C(6)	C(13)	111.0(4)
C(16)	Rh(1)	C(18)	66.0(1)	P(2)	C(7)	C(14)	112.2(3)
C(17)	Rh(1)	C(18)	36.0(1)	P(2)	C(7)	C(15)	109.3(3)
Rh(1)	P(1)	C(1)	119.0(1)	C(14)	C(7)	C(15)	109.6(4)
Rh(1)	P(1)	C(4)	112.2(1)	Rh(1)	C(16)	C(17)	73.0(2)
Rh(1)	P(1)	C(5)	117.8(1)	Rh(1)	C(17)	C(16)	68.7(2)
C(1)	P(1)	C(4)	102.4(2)	Rh(1)	C(17)	C(18)	78.3(2)
C(1)	P(1)	C(5)	99.9(2)	Rh(1)	C(17)	C(22)	115.7(2)
C(4)	P(1)	C(5)	103.2(2)	C(16)	C(17)	C(18)	119.6(3)
Rh(1)	P(2)	C(3)	118.6(2)	C(16)	C(17)	C(22)	123.6(4)
Rh(1)	P(2)	C(6)	113.0(1)	C(18)	C(17)	C(22)	116.1(3)
Rh(1)	P(2)	C(7)	116.9(1)	Rh(1)	C(18)	C(17)	65.6(2)
C(3)	P(2)	C(6)	103.0(2)	Rh(1)	C(18)	C(19)	127.0(3)
C(3)	P(2)	C(7)	99.9(2)	C(17)	C(18)	C(19)	120.6(3)
C(6)	P(2)	C(7)	103.3(2)	C(18)	C(19)	C(20)	120.6(4)
P(1)	C(1)	C(2)	115.9(3)	C(19)	C(20)	C(21)	119.9(4)
C(1)	C(2)	C(3)	113.9(3)	C(20)	C(21)	C(22)	120.8(4)
P(2)	C(3)	C(2)	115.0(3)	C(17)	C(22)	C(21)	121.8(4)
P(1)	C(4)	C(8)	109.8(3)				

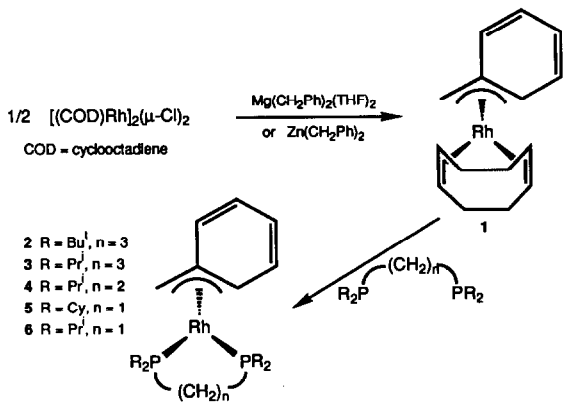

Scheme 1.

ters, bond lengths, and bond angles are given in Tables 2–4, respectively. Hydrogen atom parameters, anisotropic thermal parameters, torsion angles, intermolecular contacts, least-squares planes, and measured and calculated structure factor amplitudes are available from the authors.

3. Results and discussion

3.1. Benzyl complexes

In a previous report [24], the synthesis of η^3-allylic complexes of rhodium was achieved by the addition of freshly prepared solutions of simple allyl Grignard reagents to $[(COD)Rh]_2(\mu\text{-}Cl)_2$. The use of $Zn(CH_2Ph)_2$ or $Mg(CH_2Ph)_2(THF)_2$ to prepare $(COD)Rh(\eta^3\text{-}CH_2Ph)$ (**1**) represents an improvement since the alkylating reagents are solids which can be made on a large scale and stored indefinitely in a glovebox. $Mg(CH_2Ph)_2(THF)_2$ is the reagent of choice for large scale preparations due to the greater insolubility of $MgCl_2$ as compared to $ZnCl_2$. Compound **1** is thermally sensitive but can be stored at −40°C under nitrogen for several months with little decomposition. The COD ligand in **1** can be displaced with bulky chelating diphosphines, generating the thermally stable η^3-benzylic compounds **2–6** (Scheme 1). It turns out that the diphosphine η^3-benzyl derivatives are superior to the allyl analogs because the hydrogenolysis of these species is easier; for example $\{^iPr_2P(CH_2)_3P^iPr_2\}Rh(\eta^3\text{-}C_3H_5)$ requires 48 h to go to completion, whereas the hydrogenolysis of $\{^iPr_2P(CH_2)_3P^iPr_2\}Rh(\eta^3\text{-}CH_2Ph)$ (**3**) only takes 2 h under identical conditions of pressure and concentration. The rhodium benzyl complexes **1–6** are soluble in common organic solvents and crystallize easily.

The ^1H NMR spectrum of **1** shows two resonances for the COD olefinic protons indicating that the benzylic carbon remains *trans* to one of the coordinated olefins of COD. This is consistent with the $^{13}C\{^1H\}$ NMR spectrum which shows two resonances for the olefinic carbons of the COD ligand.

The $^{31}P\{^1H\}$ NMR spectra of the rhodium benzyl complexes **2–6** reveal a characteristic first order AMX pattern, that is indicative of mononuclear species with inequivalent phosphorus donors coupled to rhodium-103. This is consistent with the molecular weight [25] of 450 found for complex $(dippm)Rh(\eta^3\text{-}CH_2Ph)$ (**6**) (calc. 442). The AMX $^{31}P\{^1H\}$ NMR pattern for $(dippp)Rh(\eta^3\text{-}CH_2Ph)$ (**3**) is maintained from 80°C to −103°C, indicating that no exchange process of the phosphines is occurring within this temperature range. The coupling constants of $^1J(P,Rh)$ and $^2J(P,P')$ did not change over this temperature range, in contrast to that reported for $[(^iPrO)_3P]_2Rh\{\eta^3\text{-}CH_2C_6(CH_3)_5\}$ [2]. At high temperature, the benzyl ligand may adopt a η^1-coordination but this does not equate the phosphines. This is in agreement with known three-coordinate bis(phosphine) complexes [26,27] which adopt a bent "T" shaped structure.

The $^{13}C\{^1H\}$ NMR spectra of the rhodium benzyl compounds **1–6** show a shift to higher field for the *ortho* and *ipso* carbons of the benzyl fragment, with respect to $\eta^1\text{-}CH_2Ph$, due to the interaction with the rhodium centre. No change was observed in the $^{13}C\{^1H\}$ spectrum of $(dippp)Rh(\eta^3\text{-}CH_2Ph)$ down to −90°C. A characteristic doublet for the *ortho* carbon of rhodium benzyl complexes **2–6** is interpreted as coupling to the *trans* phosphine and not to rhodium since this doublet is absent in **1** (COD ligand donor). The benzylic carbon of the diphosphine complexes **2–6** appears as a multiplet with $^1J(C,Rh)$ of the order of 10 Hz, consistent with the simple doublet of 10.9 Hz observed for **1**. A strong two-bond coupling (~ 30 Hz) to the *trans* phosphine is also seen for the benzylic carbon of the diphosphine complexes **2–6**.

The ^1H NMR spectra of the rhodium benzyl complexes **1–6** are all similar with a characteristic upfield shift for the *ortho* protons of the benzyl ligand. Both *ortho* protons are equivalent and appear as a doublet resonance due to coupling to the *meta* proton of the benzyl fragment; no *ortho* proton coupling to rhodium was observed for any of the complexes. With the exception of broadening, there was no change in the ^1H NMR of $(dippp)Rh(\eta^3\text{-}CH_2Ph)$ down to −70°C. The benzylic protons of the rhodium benzyl complexes **2–6** appear as doublets with a strong three-bond *trans* coupling to phosphorus of about 7 Hz. Previously, this has been interpreted as a two-bond proton-rhodium coupling in the analogous complex $[(^iPrO)_3P]_2Rh\{\eta^3\text{-}CH_2C_6\text{-}(CH_3)_5\}$ [2], but since the benzylic protons in $(COD)Rh(\eta^3\text{-}CH_2Ph)$ appear as a singlet, it is likely *trans* phosphorus-proton coupling. The ^1H and $^{13}C\{^1H\}$ NMR data above suggest that the benzyl ligand in all

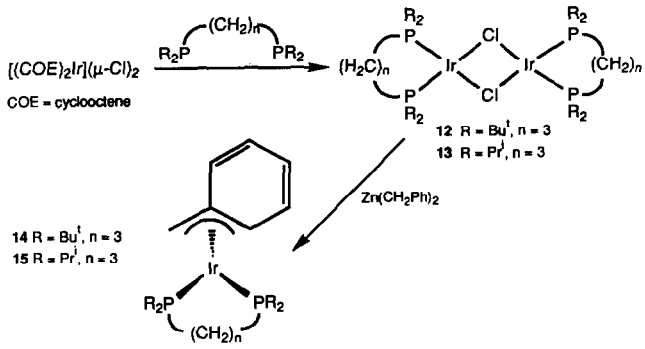

Scheme 2.

of the complexes, **1–6**, is undergoing a rapid suprafacial exchange [10] which remains fast on the NMR time scale in the temperature region studied.

The preparation of (COD)Ir(η^3-C_3H_5) has previously been reported by the low temperature addition of Li(C_3H_5) to [(COD)Ir]$_2$(μ-Cl)$_2$ [28]; due to its thermal instability, this iridium allyl derivative was not isolated but rather used *in situ*. Anticipating the instability of the analogous complex (COD)Ir(η^3-CH_2Ph), the diphosphines were introduced first before incorporation of the benzyl moiety. The addition of 2 equiv. of a diphosphine ligand to [(COE)$_2$Ir]$_2$(μ-Cl)$_2$ yields the extremely air-sensitive complexes [P_2Ir]$_2$(μ-Cl)$_2$ (P_2 = dtbpp and dippp) (see Scheme 2, below). Only the complexes **12** and **13** having diphosphines with a three carbon backbone, have been prepared in pure form; for the chelating ligands dippe, dcypm and dippm, complex mixtures result. The addition of Zn(CH_2Ph)$_2$ to the diphosphine iridium chloro-bridged dimers leads to the desired η^3-benzyl compounds in high yield. The iridium benzyl complexes **14** and **15** are quite thermally stable. Similar shifts for the benzyl moiety are observed in the ^{1}H and ^{13}C{^{1}H} NMR spectra as found for the rhodium analogs. The two doublets at 27.0 and 21.4 ppm observed in the ^{31}P{^{1}H} NMR spectrum of (dippp)Ir(η^3-CH_2Ph) confirms the rigid η^3-coordination of the benzyl ligand.

3.2. Solid state structure of (dippp)Rh(η^3-CH_2Ph)

The molecular structure of {^{i}Pr$_2$P(CH_2)$_3$P^{i}Pr$_2$}-Rh(η^3-CH_2Ph) (**3**) is shown in Fig. 1. The ligands adopt a nearly square planar arrangement around the rhodium centre using the *ortho* carbon as the fourth site. The rhodium–phosphorus(P1) bond *trans* to the benzylic carbon is longer than the rhodium-phosphorus(P2) bond *cis*, by 0.045 Å, probably due to a greater steric interaction with the phenyl portion of the benzyl ligand, as well as a greater σ-donation from the benzylic carbon. The carbon–rhodium bond lengths in the benzyl fragment increase in the order Rh–C(16) > Rh–C(17) > Rh–C(18), owing to the larger amount of electron density on the benzylic carbon and the weak carbon–metal interaction of the phenyl portion of the benzyl fragment. The aromaticity of the phenyl ring has been disturbed with localization of double bonds between C19 and C20, and C21 and C22. The bond lengths C16–C17 and C17–C18 are statistically the same due to delocalization of the π-allylic system.

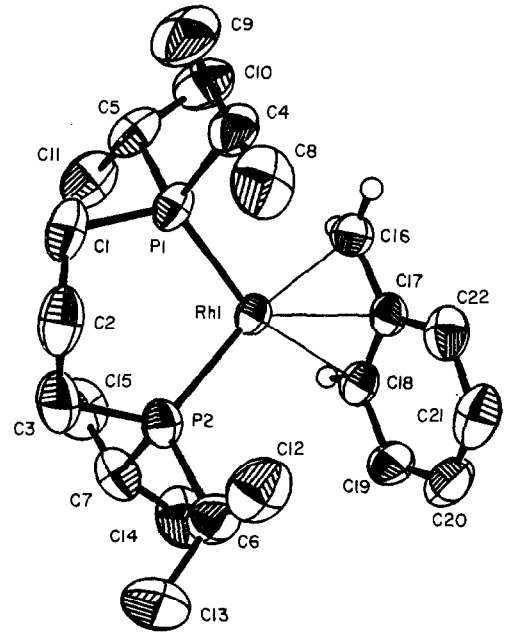

Fig. 1. ORTEP drawing of (dippp)Rh(η^3-CH_2Ph) (**3**); 50% probability thermal ellipsoids are shown for the non-hydrogen atoms.

3.3. Hydride complexes

The coordinatively unsaturated rhodium benzyl complexes **2–6** all react with hydrogen rapidly at −80°C without the buildup of intermediates, as monitored by ^{31}P{^{1}H} NMR spectroscopy. Complexes **2–4** give the dihydride dimers, **7–9** (eqn. (1)), wherein the diphosphine is chelating on each rhodium centre. The binuclear dihydrides **8** and **9** have been reported previously [11,12]. The binuclearity of hydride **7**, having ^{t}Bu substituents at phosphorus, was determined in solution by

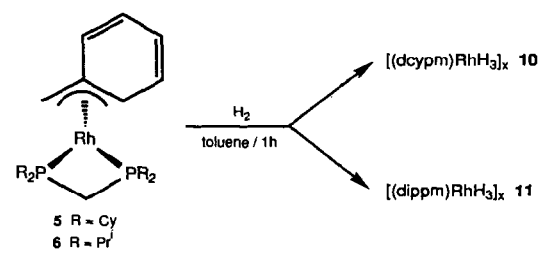

Scheme 3.

the multiplicity of the bridging hydride pattern in the ^{1}H NMR spectrum. The quintet of triplets pattern is ascribed to coupling to two equivalent rhodium-103 nuclei and four equivalent ^{31}P nuclei. This binuclear hydride derivative, $[(dtbpp)Rh]_2(\mu\text{-}H)_2$ (**7**) is soluble in THF, sparingly soluble in aromatic solvents and insoluble in aliphatic solvent.

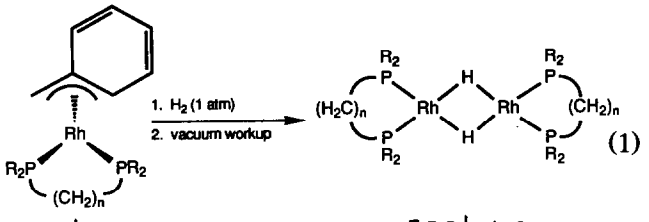

Attempts to prepare iridium hydrides by hydrogenolysis of the iridium benzyl complexes **14** and **15** were unsuccessful as only inseparable mixtures of products were produced as evidenced by ^{1}H and ^{31}P{^{1}H} NMR spectroscopy.

The rhodium η^3-benzyl complexes **5** and **6** also react with H_2 (1 atm) to generate hydride complexes with a completely different structure than that indicated in eqn. (1) (see Scheme 3). This is evident from the ^{31}P NMR spectra of $[(dcypm)RhH_3]_x$ (**10**) and $[(dippm)RhH_3]_x$ (**11**) which show a much reduced phosphorus–rhodium coupling constant, indicative of a Rh^{III} species [29,30]; the ^{31}P{^{1}H} NMR spectrum of **11** is shown in Fig. 2. The hydride derivatives **10** and **11** form deep red–black solutions in toluene, in contrast to the binuclear dihydride dimers **7–9**, which form dark green solutions. In solution, complex **10**, having cyclohexyl substituents at phosphorus, loses hydrogen readily under a vacuum to yield a single insoluble product whose structure is as yet undetermined; however, solutions of $[(dippm)RhH_3]_x$ (**11**) are quite stable in toluene or aliphatic hydrocarbons but do slowly lose hydrogen over many months in benzene. In the solid state, **11** is indefinitely stable.

The ^{1}H NMR spectrum of **11** shows two multiplets in the hydride region at -10.92 ppm and -14.88 ppm in the ratio of 2:4 with respect to the ligand resonances (assuming a binuclear structure). In the tetrahydride complex $[\{(Me_2N)_3P\}_2RhH_2](\mu\text{-}H)_2[Rh\{P(NMe_2)_3\}_2]$ [31] (**II**), which contains both bridging and terminal hydrides in the same plane, the bridging hydrides resonate at -10.5 ppm and the terminal at -16.8 ppm.

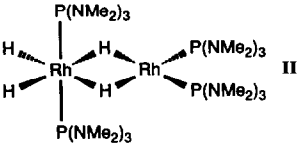

Interestingly, in **II** the rhodium centre that contains the *trans* disposed phosphines also exhibits the higher coordination number. Both ^{1}H{^{31}P} and selective ^{1}H homonuclear decoupling experiments were utilized to determine how the diphosphine ligands in complexes **10** and **11** bind to the rhodium centres (binucleating **A**

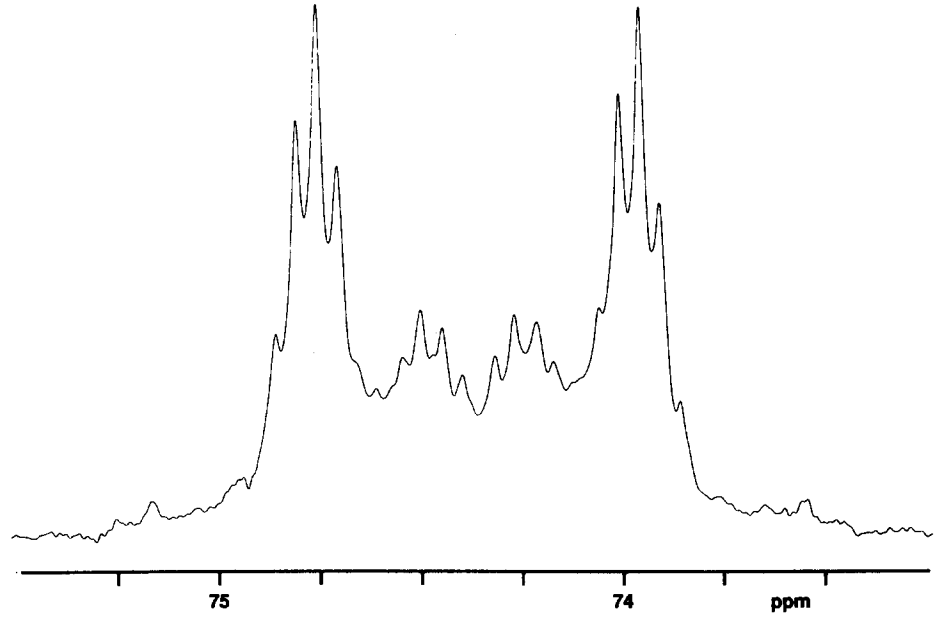

Fig. 2. ^{31}P{^{1}H} NMR spectrum for $[RhH_2]_2(\mu\text{-}H)_2(\mu\text{-dippm})_2$ (**11**).

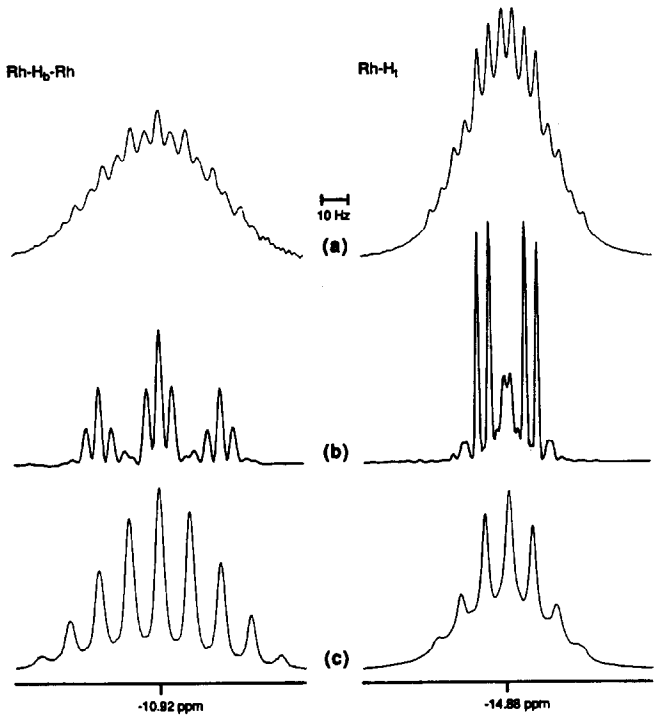

Fig. 3. ^{1}H and ^{31}P decoupling experiments for $[RhH_2]_2(\mu\text{-}H)_2(\mu\text{-di-ppm})_2$ (**11**); (a) normal ^{1}H NMR spectrum of the hydride region; (b) $^1H\{^{31}P\}$ NMR spectrum of the hydrides; (c) homonuclear decoupled ^{1}H NMR spectrum of the bridging and terminal hydrides (observe the bridging while decoupling the terminal and *vice versa*.

vs. chelating **B**). The results of the decoupling experiments are shown in Fig. 3.

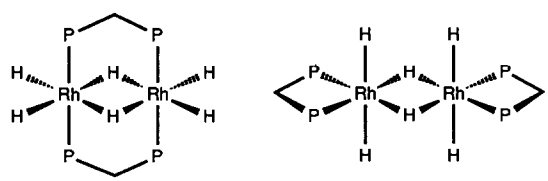

A **B**

In the $^1H\{^{31}P\}$ NMR spectrum of $[(dippm)RhH_3]_x$ (**11**), the signal at -10.92 ppm was reduced to a simple triplet of pentets due to coupling to two equivalent rhodium nuclei and four terminal hydrides, and is assigned to the bridging hydrides; the coupling to two ^{103}Rh nuclei confirms the binuclear structure of **11**. This is in accord with the molecular weight [25] of 722 found for $[(dippm)RhH_3]_2$ (**11**) (calc. 708). This simple coupling pattern is most easily accommodated by a rigid structure such as **B**. Alternatively, if **A** (binucleating) is assumed to be rigid, a second-order pattern would be expected for the bridging hydride providing $^2J(H,H)_{cis}$ is quite different from $^2J(H,H)_{trans}$. However, *cis* and *trans* hydride couplings are generally quite small (2–7 Hz) or absent [32,33] and therefore it is possible that $^2J(H,H)_{cis} \cong {}^2J(H,H)_{trans}$. The signal for the terminal hydrides at -14.88 ppm remained as a second order pattern in the $^1H\{^{31}P\}$ NMR spectrum, probably due to long range coupling to rhodium. This is consistent for both structures **A** and **B**. The rigid nature of complex **11** is supported by the absence of any exchange between the hydrides from -50°C to $+70$°C.

Differentiation of the two possible structures **A** and **B** comes from the phosphorus coupled ^{1}H NMR spectrum. Decoupling of the terminal hydrides at -14.88 ppm reduces the bridging hydrides multiplet at -10.92 ppm to an overlapping triplet of pentets ($^1J(H,Rh) = 24.5$ Hz; $^2J(H,P) = 12.2$ Hz). Coupling constants in this range are very common for other binucleating structures of rhodium which contain bridging hydrides [34–36]. Decoupling of the bridging hydrides at -10.92 ppm reveals a second order pattern for the terminal hydrides at -14.88 ppm. A second order pattern would be expected for the terminal hydrides if the phosphines in structure **A** are all strongly coupled, whereas structure **B** would most likely lead to a more simplified pattern. Additional support for structure **A** is the $^{31}P\{^1H\}$ NMR spectrum of **11** shown in Fig. 2 which is significantly different from that observed for the dihydride dimers **7–9**. So far we have been unable to simulate any of the hydride patterns or the phosphorus NMR spectra of these complexes.

Based on the above data, and in the absence of an X-ray structure, structure **A** is the most likely for the hydride complexes incorporating the one carbon backbone diphosphines. Although axial–axial interactions are extensive in binucleating structures, and likely more pronounced with bulky alkyl substituents such as isopropyl or cyclohexyl, we believe this mode of coordination is responsible for the observed binuclear hydrides. Referring back to $[\{(Me_2N)_3P\}_2RhH_2](\mu\text{-}H)_2[Rh\{P(NMe_2)_3\}_2]$ (**II**), the *trans* disposed nature of the phosphines on the octahedrally coordinated rhodium(III) centre would seem to provide the correct ligand arrangement for the stabilization of a trihydride species. Further, addition of dihydrogen to **II** is not possible since the remaining *cis*-coordinated phosphines cannot move into axial sites due to steric crowding. Indeed, mononuclear trihydride complexes such as $(^tBu_3P)_2RhH_3$ [37], which contain *trans* disposed bulky phosphines, have been prepared from $(^tBu_3P)_2RhH$ and H_2. The ligands $^iPr_2PCH_2P^iPr_2$ (dippm) and $Cy_2PCH_2PCy_2$ (dcypm) provide the essential steric bulk and diaxial coordination of the phosphines required for the formation of stable binuclear hexahydride complexes. It is interesting to note the existence of the isoelectronic iridium analogue [38], **III**, which is two hydrides removed from the hexahydride structures re-

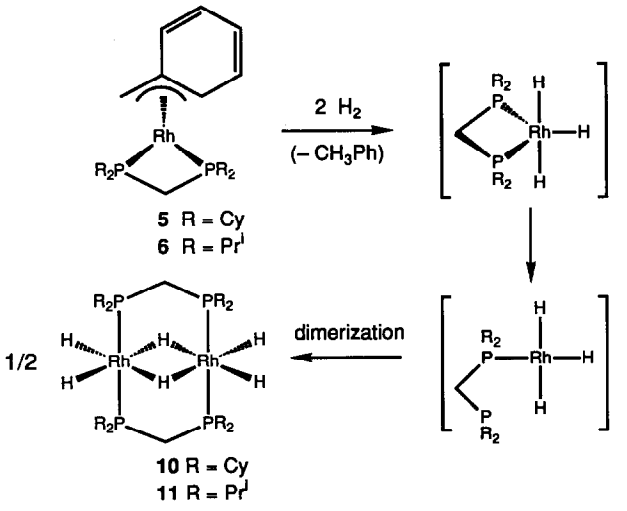

Scheme 4.

ported herein. The difficulty in removing the two remaining carbonyl ligands has likely rendered hexahydride complexes inaccessible from this particular complex.

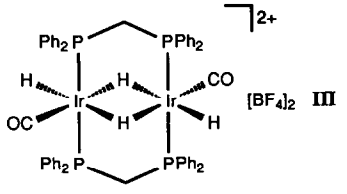

III

A mechanism for the formation of the binuclear hexahydride complexes **10** and **11** is difficult to substantiate since no intermediates are observed. Nonetheless, several important features are worth noting (Scheme 4). The hydrogenolysis of the mononuclear complexes $P_2Rh(\eta^3\text{-}CH_2Ph)$ (P_2 = dcypm **5** and dippm **6**) proceeds cleanly to give only one phosphorus containing compound by $^{31}P\{^1H\}$ NMR spectroscopy. Furthermore, the four membered chelate ring is likely to be labile due to ring strain which may facilitate phosphine dissociation [39] at some key step in the hydrogenation. The bridging coordination geometry of the diphosphine certainly relieves this ring strain and likely leads to the much more stable binuclear hexahydride structure **A**.

4. Conclusion

The straightforward synthesis and characterization of the above mentioned complexes has provided a facile route for the production of diphosphine benzyl derivatives of rhodium and iridium. The X-ray crystal structure of $\{^iPr_2P(CH_2)_3P^iPr_2\}Rh(\eta^3\text{-}CH_2Ph)$ revealed a square planar arrangement of the diphosphine and η^3-benzyl moiety about the rhodium centre. For the mononuclear complexes of the general formula $P_2Rh(\eta^3\text{-}CH_2Ph)$ ($P_2 = {}^tBu_2P(CH_2)_3P^tBu_2$, $^iPr_2P(CH_2)_3P^iPr_2$ and $^iPr_2P(CH_2)_2P^iPr_2$), binuclear dihydride derivatives, $[P_2Rh]_2(\mu\text{-}H)_2$, are formed. New binuclear hexahydride complexes $[RhH_2]_2(\mu\text{-}H)_2(\mu\text{-}P_2)_2$, incorporating a binucleating diphosphine, are formed when the mononuclear compounds $P_2Rh(\eta^3\text{-}CH_2Ph)$ (P_2 = dippm, $^iPr_2PCH_2P^iPr_2$ and dcypm, $Cy_2PCH_2PCy_2$) are hydrogenated. The reactivity of these new binuclear hexahydride complexes and how they differ from the dihydride species will be the subject of a future publication.

References

1 K. S. Y. Lau, Y. Becker, F. Huang, N. Baenziger and J. K. Stille, *J. Am. Chem. Soc., 99* (1977) 5664.
2 R. R. Burch, E. L. Muetterties and V. W. Day, *Organometallics, 1* (1982) 188.
3 H. O. Stuehler and H. Pickardt, *Z. Naturforsch., 36B* (1981) 315.
4 H. O. Stuehler, *Angew. Chem., 92* (1980) 475.
5 M. Takesada, H. Yamazaki and N. Hagihara, *Nippon Kagaku Zasshi, 89* (1968) 1121.
6 L. E. Crascall, S. A. Litster, A. D. Redhouse and J. L. Spencer, *J. Organomet. Chem., 394 (1990) C35.*
7 R. B. King and A. Fronzaglia, *J. Am. Chem. Soc., 88* (1966) 709.
8 Y. Becker and J. K. Stille, *J. Am. Chem. Soc., 100* (1978) 845.
9 J. S. Roberts and K. J. Klabunde, *J. Am. Chem. Soc., 99* (1977) 2509.
10 F. A. Cotton and T. J. Marks, *J. Am. Chem. Soc., 91* (1969) 1339.
11 M. D. Fryzuk, W. E. Piers, F. W. B. Einstein and T. Jones, *Can. J. Chem., 67* (1989) 883.
12 M. D. Fryzuk, T. Jones and F. W. B. Einstein, *Organometallics, 3* (1984) 185.
13 M. D. Fryzuk, L. Rosenberg and S. J. Rettig, *Organometallics 10.* (1991) 2537.
14 M. D. Fryzuk, *Organometallics, 9* (1990) 1359.
15 M. D. Fryzuk, W. E. Piers, S. J. Rettig, T. Jones, F. W. B. Einstein and T. S. Albright, *J. Am. Chem. Soc., 111* (1989) 5709.
16 M. D. Fryzuk and W. E. Piers, *Polyhedron, 7* (1988) 1001.
17 J. Chatt and L. M. Venanzi, *J. Chem. Soc.*, (1957) 4753.
18 A. Van Der Ent and A. L. Onderlinden, *Inorg. Synth., 14* (1973) 94.
19 R. R. Schrock, *J. Organomet. Chem., 122* (1976) 209.
20 K. Tani, E. Tanigawa, Y. Tatsubo and S. Otsuka, *J. Organomet. Chem., 279* (1985) 87.
21 Z. S. Novikova, A. A. Prishchenko and I. F. Lutsenko, *J. Gen. Chem. USSR*, (1977) 707.
22 TEXSAN/TEXRAY structure analysis package which includes versions of the following: DIRDIF, direct methods for difference structures, by P. T. Beurskens; ORFLS, full-matrix least-squares, and ORFFE, function and errors, by W. R. Busing, K. O. Martin, and H. A. Levy; ORTEP II, illustrations, by C. K. Johnson.
23 *International Tables for X-Ray Crystallography*, Vol. IV, Kynoch, Birmingham, 1974, pp. 99–102 and 149.
24 M. D. Fryzuk and W. E. Piers, *Organomet. Synth., 3* (1986) 128.
25 E. P. Clark, Indust. *Eng. Chem., Anal. Chem., 13* (1941) 820.
26 H. L. M. Van Gaal and F. L. A. Van Den Bekerom, *J. Organomet. Chem., 134* (1977) 237.
27 T. Yoshida, T. Okano and S. Otsuka, *J. Organomet. Chem., 134* (1978) 237.

28 E. L. Muetterties, K. D. Tau, J. F. Kirner, T. V. Harris, J. Stark, M. R. Thompson and V. W. Day, *Organometallics, 1* (1982) 1562.
29 J. F. Nixon and A. Pidcock, *Annu. Rev. NMR Spectrosc., 2* (1969) 345.
30 D. W. Meek and T. J. Mazanec, *Acc. Chem. Res., 14* (1981) 266.
31 E. C. Meier, R. R. Burch, E. L. Muetterties and V. W. Day, *J. Am. Chem. Soc., 104* (1982) 2661.
32 M. D. Fryzuk and P. A. MacNeil, *Organometallics, 2* (1983) 682.
33 B. E. Mann, C. Masters and B. L. Shaw, *J. Chem. Soc., Chem. Commun.*, (1970) 846.
34 D. M. Antonelli and M. Cowie, *Inorg. Chem., 29* (1990) 4039.
35 R. MacDonald and M. Cowie, *Inorg. Chem., 29* (1990) 1564.
36 C. Woodcock and R. Eisenberg, *Inorg. Chem., 23* (1984) 4207.
37 T. Oshida, T. Okano, D. L. Thorn, T. H. Tulip, S. Otsuka and J. A. Ibers, *J. Organomet. Chem., 181* (1979) 183.
38 R. MacDonald, B. R. Sutherland and M. Cowie, *Inorg. Chem., 26* (1987) 3333.
39 D. M. Antonelli and M. Cowie, *Organometallics, 9* (1990) 1818.